

# Implications of SUSY Searches at the LHC for the ILC <sup>\*</sup>

S. HEINEMEYER<sup>†</sup>

*Instituto de Física de Cantabria (CSIC-UC), Santander, Spain*

## Abstract

Global frequentist fits to the CMSSM and NUHM1 using the **MasterCode** framework are updated to include the public results of searches for supersymmetric signals using  $\sim 1/\text{fb}$  of LHC data recorded by ATLAS and CMS and  $\sim 0.3/\text{fb}$  of data recorded by LHCb. We also include the constraints imposed by the electroweak precision and B-physics observables, the cosmological dark matter density and the XENON100 search for spin-independent dark matter scattering. Finally we also investigate the impact of a possible Higgs signal around 125 GeV. The various constraints set new bounds on the parameter space of the CMSSM and the NUHM1. We discuss the impact of the new results from SUSY and Higgs searches for these bounds and analyze the impact for a future linear  $e^+e^-$  collider.

---

<sup>\*</sup>Invited talk given by S.H. at the *LCWS 2011*, September 2011, Granada, Spain

<sup>†</sup> email: Sven.Heinemeyer@cern.ch

# Implications of SUSY Searches at the LHC for the ILC

S. Heinemeyer

Instituto de Física de Cantabria (CSIC) E-39005 Santander, Spain

Global frequentist fits to the CMSSM and NUHM1 using the **MasterCode** framework are updated to include the public results of searches for supersymmetric signals using  $\sim 1/\text{fb}$  of LHC data recorded by ATLAS and CMS and  $\sim 0.3/\text{fb}$  of data recorded by LHCb. We also include the constraints imposed by the electroweak precision and B-physics observables, the cosmological dark matter density and the XENON100 search for spin-independent dark matter scattering. Finally we also investigate the impact of a possible Higgs signal around 125 GeV. The various constraints set new bounds on the parameter space of the CMSSM and the NUHM1. We discuss the impact of the new results from SUSY and Higgs searches for these bounds and analyze the impact for a future linear  $e^+e^-$  collider.

## 1 Introduction

The **MasterCode** collaboration [1–10] has reported the results of global fits to pre-LHC data [1–5] (see Ref. [11] for other works) as well as including LHC 2010 data [6–10] (see Ref. [12] for other works) in the frameworks of simplified variants of the minimal supersymmetric extension of the Standard Model (MSSM) [13] with universal supersymmetry-breaking mass parameters at the GUT scale. We consider a class of models in which R-parity is conserved and the lightest supersymmetric particle (LSP), assumed to be the lightest neutralino  $\tilde{\chi}_1^0$  [14], provides the cosmological cold dark matter [15]. The specific models studied have included the constrained MSSM (CMSSM) with parameters  $m_0$ ,  $m_{1/2}$  and  $A_0$  denoting common scalar, fermionic and trilinear soft supersymmetry-breaking parameters at the GUT scale, and  $\tan\beta$  denoting the ratio of the two vacuum expectation values of the two Higgs fields. Other models studied include a model in which common supersymmetry-breaking contributions to the Higgs masses are allowed to be non-universal (the NUHM1), a very constrained model in which trilinear and bilinear soft supersymmetry-breaking parameters are related (the VCMSSM), and minimal supergravity (mSUGRA) in which the gravitino mass is required to be the same as the universal soft supersymmetry-breaking scalar mass before renormalization (see Ref. [8] for an extensive list of references for those models).

The impressive increase in the accumulated LHC luminosity combined with the rapid analyses of LHC data by the ATLAS [16, 17], CMS [18–20] and LHCb Collaborations [21] have been included in the analysis presented in Ref. [8]. Most recently, the ATLAS and CMS Collaborations have presented preliminary updates of their results for the search for a SM-like Higgs boson with  $\sim 5/\text{fb}$  of data [22]. These results may be compatible with a SM-like Higgs boson around  $M_h \simeq 125$  GeV, and they have been included in the analysis presented in Ref. [9].

Here we review the results of Refs. [8, 9], which are focused on the CMSSM and the NUHM1. We discuss their impact on the physics prospects for a future linear  $e^+e^-$  collider, in particular the ILC, with a center-of-mass energy around 1 TeV (the ILC(1000)).

## 2 The MasterCode framework

We define a global  $\chi^2$  likelihood function, which combines all theoretical predictions with experimental constraints (except the latest LHC SUSY and Higgs searches):

$$\chi^2(\equiv \chi_{\text{org}}^2) = \sum_i^N \frac{(C_i - P_i)^2}{\sigma(C_i)^2 + \sigma(P_i)^2} + \sum_i^M \frac{(f_{\text{SM}_i}^{\text{obs}} - f_{\text{SM}_i}^{\text{fit}})^2}{\sigma(f_{\text{SM}_i})^2} + \chi^2(M_h) + \chi^2(\text{BR}(B_s \rightarrow \mu\mu)) . \quad (1)$$

Here  $N$  is the number of observables studied,  $C_i$  represents an experimentally measured value (constraint) and each  $P_i$  defines a prediction for the corresponding constraint that depends on the supersymmetric parameters. The experimental uncertainty,  $\sigma(C_i)$ , of each measurement is taken to be both statistically and systematically independent of the corresponding theoretical uncertainty,  $\sigma(P_i)$ , in its prediction. We denote by  $\chi^2(M_h)$  and  $\chi^2(\text{BR}(B_s \rightarrow \mu^+\mu^-))$  the  $\chi^2$  contributions from the two measurements for which only one-sided bounds were previously included.

We stress that the three SM parameters  $f_{\text{SM}} = \{\Delta\alpha_{\text{had}}, m_t, M_Z\}$  are included as fit parameters and allowed to vary with their current experimental resolutions  $\sigma(f_{\text{SM}})$ . We do not include  $\alpha_s$  as a fit parameter, which would have only a minor impact on the analysis.

Formulating the fit in this fashion has the advantage that the  $\chi^2$  probability,  $P(\chi^2, N_{\text{dof}})$ , properly accounts for the number of degrees of freedom,  $N_{\text{dof}}$ , in the fit and thus represents a quantitative and meaningful measure for the “goodness-of-fit.” In previous studies [1],  $P(\chi^2, N_{\text{dof}})$  has been verified to have a flat distribution, thus yielding a reliable estimate of the confidence level for any particular point in parameter space. All confidence levels for selected model parameters are performed by scanning over the desired parameters while minimizing the  $\chi^2$  function with respect to all other model parameters. The function values where  $\chi^2(x)$  is found to be equal to  $\chi_{\text{min}}^2 + \Delta\chi^2$  determine the confidence level contour. For two-dimensional parameter scans we use  $\Delta\chi^2 = 2.23(5.99)$  to determine the 68%(95%) confidence level contours. Only experimental constraints are imposed when deriving confidence level contours, without any arbitrary or direct constraints placed on model parameters themselves. This leads to robust and statistically meaningful estimates of the total 68% and 95% confidence levels, which may be composed of multiple separated contours.

The experimental constraints used in our analyses are listed in Table 2 in [8]. It should be noted that we use of the  $e^+e^-$  determination of the SM contribution to  $(g-2)_\mu$  [23],  $a_\mu^{\text{SUSY}} = (30.2 \pm 8.8) \times 10^{-10}$ . Indeed, the  $(g-2)_\mu$  hint has even strengthened with the convergence of the previously discrepant SM calculations using low-energy  $e^+e^-$  and  $\tau$  decay data [23, 24].

The numerical evaluation of the frequentist likelihood function using the constraints has been performed with the **MasterCode** [1–10], which includes the following theoretical codes. For the RGE running of the soft SUSY-breaking parameters, it uses **SoftSUSY** [25], which is combined consistently with the codes used for the various low-energy observables. At the electroweak scale we have included various codes: **FeynHiggs** [26] is used for the evaluation of the Higgs masses and  $a_\mu^{\text{SUSY}}$  (see also [27–30]). For flavor-related observables we use **SuFla** [31] as well as **SuperIso** [32], and for the electroweak precision data we have included a code based on [33]. Finally, for dark-matter-related observables, **MicrOMEGAs** [34] and **SSARD** [35] have been used. We made extensive use of the SUSY Les Houches Accord [36] in the combination of the various codes within the **MasterCode**.

The `MasterCode` framework is such that new observables can easily be incorporated via new ‘afterburners’, as we discuss below for the  $\text{LHC}_{1/\text{fb}}$  constraints. We use a Markov Chain Monte Carlo (MCMC) approach to sample the parameter spaces of supersymmetric models. The sampling is based on the Metropolis-Hastings algorithm, with a multi-dimensional Gaussian distribution as proposal density. The width of this distribution is adjusted during the sampling, so as to keep the MCMC acceptance rate between 20% and 40% in order to ensure efficient sampling. It should be noted that we do not make use of the sampling density to infer the underlying probability distribution. The results of Refs. [8, 9] are based on a basic resampling of the CMSSM with  $7 \cdot 10^7$  points and a resampling of the NUHM1 with  $7 \cdot 10^7$  additional points, both extending up to  $m_0, m_{1/2} = 4$  TeV. We check that the afterburners we apply do not shift the likelihood distributions outside the well-sampled regions.

### 3 SUSY searches at the LHC

The updates concerning SUSY searches in Ref. [8] are based on the public results of searches for supersymmetric signals using  $\sim 1/\text{fb}$  of LHC data analyzed by the ATLAS and CMS Collaborations and  $\sim 0.3/\text{fb}$  of data analyzed by the LHCb Collaboration. For our purposes, some of the most important constraints are provided by the ATLAS [16] and CMS [18] searches for jets +  $\cancel{E}_T$  events without leptons, as well as searches for the heavier MSSM Higgs bosons,  $H/A$  [17, 19]. Also important are the new upper limits on  $\text{BR}(B_s \rightarrow \mu^+ \mu^-)$  from the CMS [20], LHCb [21] and CDF Collaborations [37], which are incorporated in Ref. [8].

The CMS and ATLAS Collaborations have both announced new exclusions in the  $(m_0, m_{1/2})$  plane of the CMSSM based on searches for events with jets +  $\cancel{E}_T$  unaccompanied by charged leptons, assuming  $\tan \beta = 10$ ,  $A_0 = 0$  and  $\mu > 0$ . The updated CMS  $\alpha_T$  analysis is based on  $1.1/\text{fb}$  of data [18], and the updated ATLAS 0-lepton analysis is based on  $1.04/\text{fb}$  of data [16]. It is known that 0-lepton analyses are in general relatively insensitive to the  $\tan \beta$  and  $A_0$  parameters of the CMSSM, as has been confirmed specifically for the CMS  $\alpha_T$  analysis, and they are also insensitive to the amount of Higgs non-universality in the NUHM1. Therefore, we treat these analyses as constraints in the  $(m_0, m_{1/2})$  planes of the CMSSM and NUHM1 that are independent of the other model parameters.

The CMS and ATLAS 0-lepton searches are most powerful in complementary regions of the  $(m_0, m_{1/2})$  plane. Along each ray in this plane, we compare the expected CMS and ATLAS sensitivities, select the search that has the stronger expected 95% CL limit, and apply the constraint imposed by that search<sup>1</sup>. This subsequent evaluation/application of additional/new  $\chi^2$  contributions is called the ‘afterburner’. We assign  $\Delta\chi^2 = 5.99$ , corresponding to 1.96 effective standard deviations, along the CMS and ATLAS 95% 0-lepton exclusion contours in the  $(m_0, m_{1/2})$  plane. In the absence of more complete experimental information, we approximate the impact of these constraints by assuming that event numbers scale along rays in this plane  $\propto \mathcal{M}^{-4}$  where  $\mathcal{M} \equiv \sqrt{m_0^2 + m_{1/2}^2}$ , as described in [7]. We then use these numbers to calculate the effective numbers of standard deviations and corresponding values of  $\Delta\chi^2$  at each point in the plane. This procedure has been validated by comparing the likelihood it yields with results obtained independently using the generic

---

<sup>1</sup>It would also facilitate the modelling of LHC constraints on supersymmetry if the results from different Collaborations were combined officially, as was done at LEP, is already done for  $\text{BR}(B_s \rightarrow \mu^+ \mu^-)$  searches, and is planned for Higgs searches.

detector simulation code **DELPHES**, which has also been shown to reproduce quite accurately the likelihood function evaluated by the CMS Collaboration using their data [38].

## 4 Searches for a SM-like Higgs boson at the LHC

Within the supersymmetric frameworks discussed here, a confirmation of the excess reported by ATLAS and CMS [22] and consequently the discovery of a SM-like Higgs boson is expected to be possible during this year, with a mass in the range between 114 and 130 GeV [22]. We assume that this measurement will yield a nominal value of  $M_h$  within this range, with an experimental error that we estimate as  $\pm 1$  GeV. In Ref. [9] the possibility that the LHC experiments confirm the excess reported around 125 GeV and indeed discover a SM-like Higgs boson was analyzed. Assuming

$$M_h = 125 \pm 1(\text{exp.}) \pm 1.5(\text{theo.}) \text{ GeV} , \quad (2)$$

this new constraint was incorporated using the ‘afterburner’ approach discussed above (see also Ref. [8]).

## 5 Results from updated SUSY fits

We now review the effects on the global likelihood functions in various CMSSM and NUHM1 parameter planes from the inclusion of the latest SUSY and Higgs search data. Below also the implications for various physics observables are studied. The  $(m_0, m_{1/2})$  planes shown in Fig. 1 are for the CMSSM (left) and NUHM1 (right). The regions preferred at the 68% CL are outlined in red, and those favoured at the 95% CL are outlined in blue. In the upper row the solid (dotted) lines include (omit) the  $\text{LHC}_{1/\text{fb}}$  data. The open green star denotes the pre-LHC best-fit point [5], whereas the solid green star indicates the new best-fit point incorporating the LHC SUSY search results. In the lower row the solid (dotted) lines include (omit) the assumed LHC Higgs constraint. The open green star denotes the pre-Higgs best-fit point [8], whereas the solid green star indicates the new best-fit point incorporating a Higgs-boson mass measurement at 125 GeV.

One can see in Fig. 1 that both new experimental results have a similar, adding up effect. The preferred regions are shifted by both new constraints to substantially larger  $m_{1/2}$  and somewhat larger  $m_0$  values. A similar effect can be observed in Fig. 2, where we show the  $(m_{1/2}, \tan \beta)$  planes in the CMSSM (left) and the NUHM1 (right), including (omitting) the  $\text{LHC}_{1/\text{fb}}$  constraints in the upper row, including (omitting) the the hypothetical LHC measurement  $M_h = 125 \pm 1$  GeV in the lower row. The preferred values of  $\tan \beta$  are shifted to substantially higher values.

The results for the  $(M_A, \tan \beta)$  planes in the CMSSM and the NUHM1 are shown in Fig. 3. Again both new experimental results show a similar effect. We observe a strong increase in the best-fit value of  $M_A$  in both models, especially in the CMSSM, where after the inclusion of the latest SUSY searches and the hypothetical Higgs signal now  $M_A \sim 1600$  GeV is preferred. However, the likelihood function varies relatively slowly in both models, as compared to the pre-LHC fits.

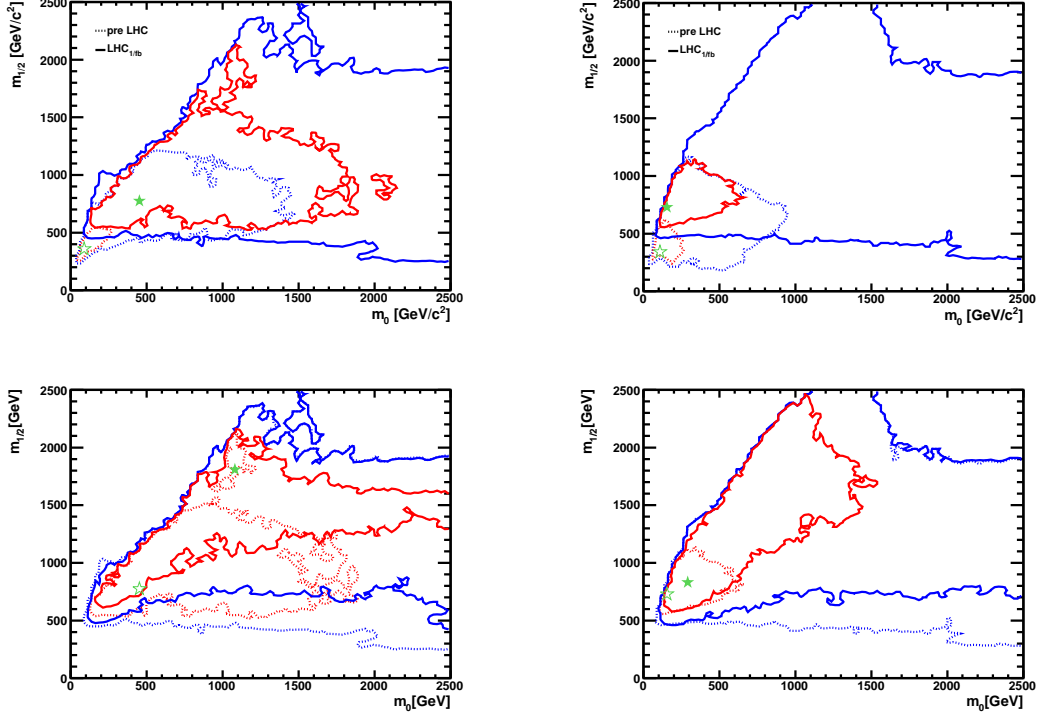


Figure 1: The  $(m_0, m_{1/2})$  planes in the CMSSM (left) and the NUHM1 (right). The  $\Delta\chi^2 = 2.30$  and  $5.99$  contours, commonly interpreted as the boundaries of the 68 and 95% CL regions, are indicated in red and blue, respectively. In the upper row the best-fit point after incorporation of the  $LHC_{1/Fb}$  constraints is indicated by a filled green star, and the pre-LHC fit [5] by an open star. The solid lines include the  $LHC_{1/Fb}$  data and the dotted lines showing the pre-LHC fits. In the lower row the solid lines include the hypothetical LHC measurement  $M_h = 125 \pm 1$  GeV and allowing for a theoretical error  $\pm 1.5$  GeV, and the dotted lines repeat the contours including the  $LHC_{1/Fb}$ , but without this  $M_h$  constraint. Here the open green stars denote the pre-Higgs best-fit points [8], whereas the solid green stars indicate the new best-fit points.

## 6 Implications for the ILC(1000)

In view of the interest in building an  $e^+e^-$  collider as the next major project at the energy frontier, we briefly review the post- $LHC_{1/Fb}$  predictions for expectations for sparticle production in  $e^+e^-$  annihilation within the CMSSM and NUHM1. In this respect it has to be kept in mind that the LHC searches are mainly sensitive to the production of coloured particles, whereas lepton colliders will have a high sensitivity in particular for the production of colour-neutral states, such as sleptons, charginos and neutralinos, as well as yielding high-precision measurements that will provide indirect sensitivity to quantum effects of new states.

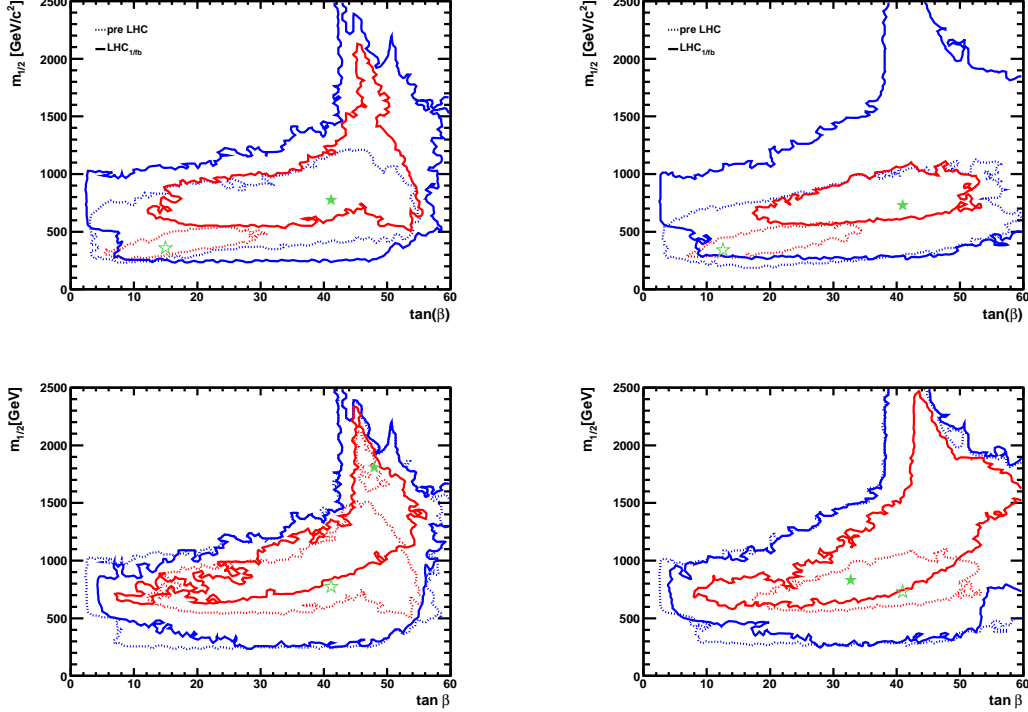


Figure 2: The  $(m_{1/2}, \tan \beta)$  planes in the CMSSM (left) and the NUHM1 (right), including (omitting) the  $LHC_{1/fb}$  constraints in the upper row, including (omitting) the hypothetical LHC measurement  $M_h = 125 \pm 1$  GeV in the lower row. The notations and significations of the contours are the same as in Fig. 1.

Fig. 4 compares the likelihood functions for various thresholds in the CMSSM (upper panel) and the NUHM1 (lower panel), based on the global fits made using the  $LHC_{1/fb}$  and XENON100 constraints. The lowest thresholds are those for  $e^+e^- \rightarrow \tilde{\chi}_1^0 \tilde{\chi}_1^0$ ,  $\tilde{\tau}_1 \tilde{\tau}_1$ ,  $\tilde{e}_R \tilde{e}_R$  and  $\tilde{\mu}_R \tilde{\mu}_R$  (the latter is not shown, it is similar to that for  $\tilde{e}_R \tilde{e}_R$ ). We see that, within the CMSSM and NUHM1, it now seems that these thresholds may well lie above 500 GeV, though in the CMSSM significant fractions of their likelihood functions still lie below 500 GeV. The thresholds for  $\tilde{\chi}_1^0 \tilde{\chi}_2^0$  and  $\tilde{e}_R \tilde{e}_L + \tilde{e}_L \tilde{e}_R$  are expected to be somewhat higher, possibly a bit below 1 TeV. The preferred value for the threshold for  $\tilde{\chi}_1^\pm \tilde{\chi}_1^\mp$  lies at about 1700 GeV in both the CMSSM and NUHM1 scenarios, that for the  $HA$  threshold lies above 1 TeV, and that for first- and second-generation squark-antisquark pair production lies beyond 2.5 TeV in both models.

### What are the implications for the ILC(1000)?

Two aspects are important for the correct interpretation of the results reviewed above with respect to the ILC(1000). First, anything inferred from the coloured sector concerning the uncoloured sector depends on the underlying model assumptions, and in particular on assumptions about the possible universality of soft supersymmetry breaking at the GUT



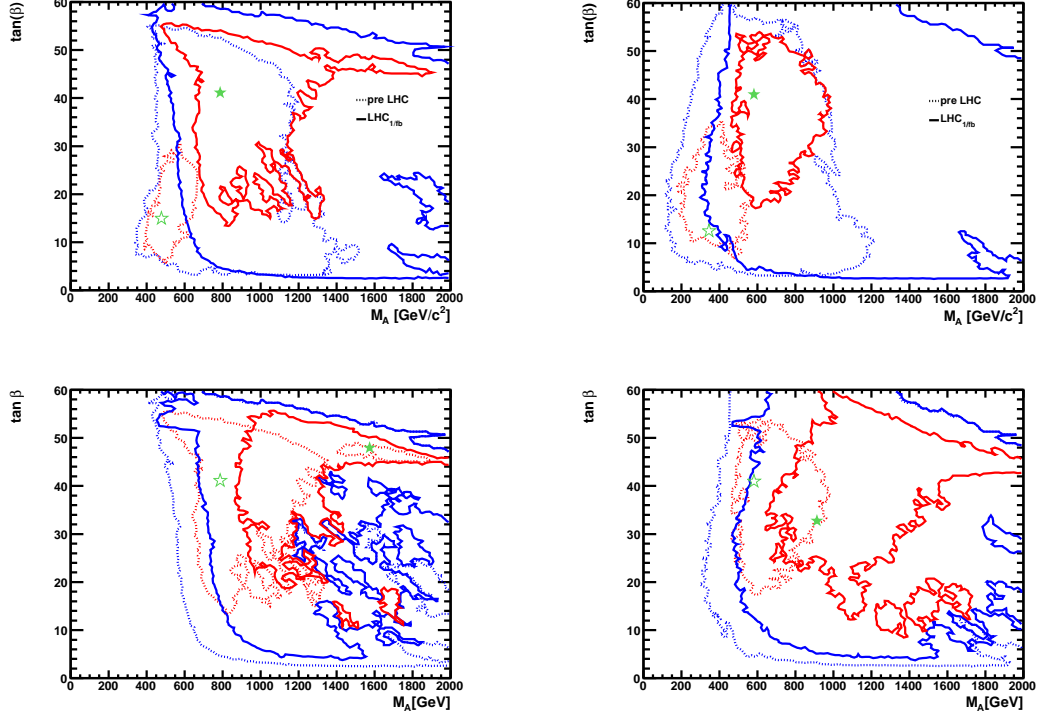


Figure 3: The  $(M_A, \tan \beta)$  planes in the CMSSM (left) and the NUHM1 (right), including (omitting) the  $LHC_{1/fb}$  constraints in the upper row, including (omitting) the hypothetical LHC measurement  $M_h = 125 \pm 1$  GeV in the lower row. The notations and significations of the contours are the same as in Fig. 1.

scale. Non-universal models, e.g., low-energy supersymmetric models, or models with different GUT assumptions, could present very different possibilities.

Second, while within the CMSSM and the NUHM1 the preferred SUSY and heavy Higgs mass ranges move to substantially higher values, this upward shift goes along with a substantial increase in  $\chi^2/\text{d.o.f.}$ , as can be seen in Tab. 1. Here we review the results for the best-fit points in the CMSSM and in the NUHM1 “pre-LHC” (i.e. no SUSY searches at the LHC, nor any assumption about any possible Higgs mass measurement), “pre-Higgs, post-LHC” (i.e. including the  $LHC_{1/fb}$  SUSY searches, but no assumption about any possible Higgs measurement) and “ $M_h \simeq 125$  GeV” (in addition the assumption of Eq. (2)). The drop in the “Fit probability” is clearly visible. The reason is that the pre-LHC data favors relatively low SUSY mass scales (to a large extent driven by  $(g - 2)_\mu$ , supported by  $M_W$  and other observables), while the non-observation of colored SUSY particles favors a heavier spectrum, leading to an increasing tension within the CMSSM and the NUHM1. Concerning the production thresholds shown in Fig. 4, further increases in the excluded regions would yield even higher thresholds, but would also make the CMSSM or NUHM1 seem even less likely. The time might come to take another look at other GUT based or non-minimal supersymmetric models, in which the colored sector (mainly searched for at



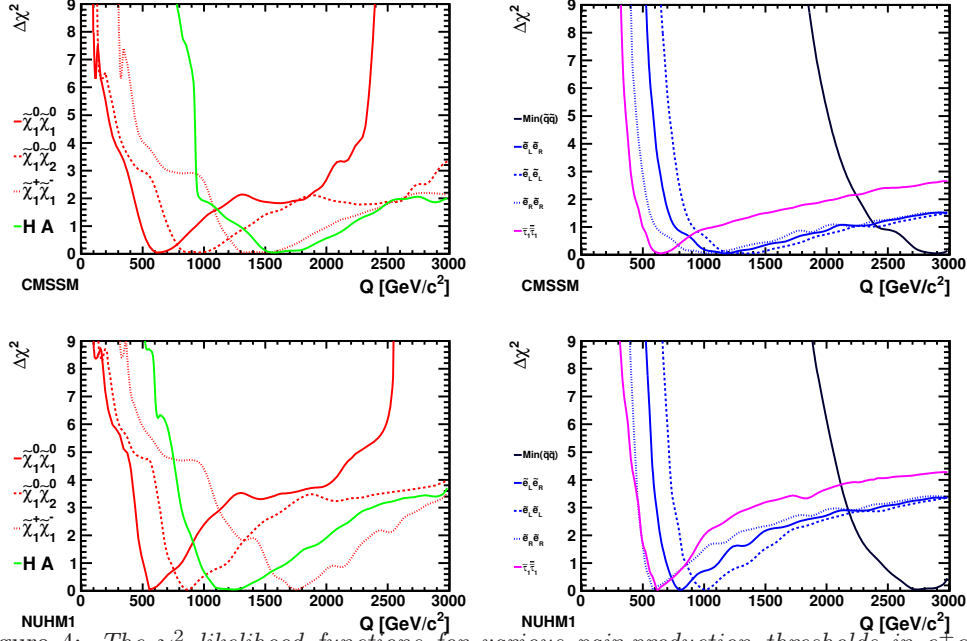


Figure 4: The  $\chi^2$  likelihood functions for various pair-production thresholds in  $e^+e^-$ , as estimated in the CMSSM (upper panel) and the NUHM1 (lower panel) after incorporating the XENON100 [39] and LHC<sub>1/fb</sub> constraints. The likelihood function for the  $\tilde{\mu}_R\tilde{\mu}_R$  threshold (not shown) is very similar to that for  $\tilde{e}_R\tilde{e}_R$ .

Model	Minimum $\chi^2/\text{d.o.f.}$	Fit Prob- ability	$m_{1/2}$ (GeV)	$m_0$ (GeV)	$A_0$ (GeV)	$\tan \beta$
CMSSM						
pre-LHC	21.5/20	37%	$360^{+180}_{-100}$	$90^{+220}_{-50}$	$-400^{+730}_{-970}$	$15^{+15}_{-9}$
pre-Higgs, post-LHC	28.8/22	15%	780	450	-1110	41
$M_h \simeq 125$ GeV	30.6/23	13%	1800	1080	860	48
NUHM1						
pre-LHC	20.8/18	29%	$340^{+280}_{-110}$	$110^{+160}_{-30}$	$520^{+750}_{-1730}$	$13^{+27}_{-6}$
pre-Higgs, post-LHC	26.9/21	17%	730	150	-910	41
$M_h \simeq 125$ GeV	29.7/22	13%	830	290	660	33

Table 1: Comparison of the best-fit points found in the CMSSM and NUHM1 pre-LHC<sub>1/fb</sub> [5], pre-Higgs [8] and including the latest results from SUSY and Higgs searches.

the LHC) and the uncolored sector (which is relevant, e.g., for  $(g-2)_\mu$ ) are less strongly connected as in the CMSSM or NUHM1.

## Acknowledgments

We thank O. Buchmueller, R. Cavanaugh, A. De Roeck, M.J. Dolan, J.R. Ellis, H. Flächer, G. Isidori, J. Marrouche, K.A. Olive, S. Rogerson, F.J. Ronga, K.J. de Vries and G. Weiglein with whom many results shown here have been obtained. We thank especially G. Moortgat-Pick for helpful discussions and important contributions to the talk. The work of S.H. is supported in part by CICYT (grant FPA 2010–22163-C02-01) and by the Spanish MICINN’s Consolider-Ingenio 2010 Program under grant MultiDark CSD2009-00064.

## References

- [1] O. Buchmueller *et al.*, Phys. Lett. B **657** (2007) 87 [arXiv:0707.3447 [hep-ph]].
- [2] O. Buchmueller *et al.*, JHEP **0809** (2008) 117 [arXiv:0808.4128 [hep-ph]].
- [3] O. Buchmueller *et al.*, Eur. Phys. J. C **64** (2009) 391 [arXiv:0907.5568 [hep-ph]].
- [4] O. Buchmueller *et al.*, Phys. Rev. D **81** (2010) 035009 [arXiv:0912.1036 [hep-ph]].
- [5] O. Buchmueller *et al.*, Eur. Phys. J. C **71** (2011) 1583 [arXiv:1011.6118 [hep-ph]].
- [6] O. Buchmueller *et al.*, Eur. Phys. J. C **71** (2011) 1634 [arXiv:1102.4585 [hep-ph]].
- [7] O. Buchmueller *et al.*, Eur. Phys. J. C **71** (2011) 1722 [arXiv:1106.2529 [hep-ph]].
- [8] O. Buchmueller *et al.*, to appear in Eur. Phys. J. C, arXiv:1110.3568 [hep-ph].
- [9] O. Buchmueller *et al.*, arXiv:1112.3564 [hep-ph].
- [10] For more information and updates, please see <http://cern.ch/mastercode/>.
- [11] For a sampling of other pre-LHC analyses, see: E. A. Baltz and P. Gondolo, JHEP **0410** (2004) 052 [arXiv:hep-ph/0407039]; B. C. Allanach and C. G. Lester, Phys. Rev. D **73** (2006) 015013 [arXiv:hep-ph/0507283]; R. R. de Austri, R. Trotta and L. Roszkowski, JHEP **0605** (2006) 002 [arXiv:hep-ph/0602028]; R. Lafaye, T. Plehn, M. Rauch and D. Zerwas, Eur. Phys. J. C **54** (2008) 617 [arXiv:0709.3985 [hep-ph]]; S. Heinemeyer, X. Miao, S. Su and G. Weiglein, JHEP **0808** (2008) 087 [arXiv:0805.2359 [hep-ph]]; R. Trotta, F. Feroz, M. P. Hobson, L. Roszkowski and R. Ruiz de Austri, JHEP **0812** (2008) 024 [arXiv:0809.3792 [hep-ph]]; P. Bechtle, K. Desch, M. Uhlenbrock and P. Wienemann, Eur. Phys. J. C **66** (2010) 215 [arXiv:0907.2589 [hep-ph]].
- [12] For a sampling of other post-LHC analyses, see: D. Feldman, K. Freese, P. Nath, B. D. Nelson and G. Peim, Phys. Rev. D **84**, 015007 (2011) [arXiv:1102.2548 [hep-ph]]; B. C. Allanach, Phys. Rev. D **83**, 095019 (2011) [arXiv:1102.3149 [hep-ph]]; S. Scopel, S. Choi, N. Fornengo and A. Bottino, Phys. Rev. D **83**, 095016 (2011) [arXiv:1102.4033 [hep-ph]]; P. Bechtle *et al.*, arXiv:1102.4693 [hep-ph]; B. C. Allanach, T. J. Khoo, C. G. Lester and S. L. Williams, JHEP **1106**, 035 (2011) [arXiv:1103.0969 [hep-ph]]; S. Akula, N. Chen, D. Feldman, M. Liu, Z. Liu, P. Nath and G. Peim, Phys. Lett. B **699**, 377 (2011) [arXiv:1103.1197 [hep-ph]]; M. J. Dolan, D. Grellscheid, J. Jaeckel, V. V. Khoze and P. Richardson, JHEP **1106**, 095 (2011) [arXiv:1104.0585 [hep-ph]]; S. Akula, D. Feldman, Z. Liu, P. Nath and G. Peim, Mod. Phys. Lett. A **26**, 1521 (2011) [arXiv:1103.5061 [hep-ph]]; M. Farina, M. Kadastik, D. Pappadopulo, J. Pata, M. Raidal and A. Strumia, Nucl. Phys. B **853**, 607 (2011) [arXiv:1104.3572 [hep-ph]]; S. Profumo, Phys. Rev. D **84**, 015008 (2011) [arXiv:1105.5162 [hep-ph]]; T. Li, J. A. Maxin, D. V. Nanopoulos and J. W. Walker, arXiv:1106.1165 [hep-ph]; N. Bhattacharyya, A. Choudhury and A. Datta, Phys. Rev. D **84**, 095006 (2011) [arXiv:1107.1997 [hep-ph]].
- [13] H. P. Nilles, Phys. Rep. **110** (1984) 1; H. E. Haber and G. L. Kane, Phys. Rept. **117** (1985) 75.
- [14] H. Goldberg, Phys. Rev. Lett. **50** (1983) 1419; J. Ellis, J. Hagelin, D. Nanopoulos, K. Olive and M. Srednicki, Nucl. Phys. B **238** (1984) 453.
- [15] E. Komatsu *et al.* [WMAP Collaboration], Astrophys. J. Suppl. **192** (2011) 18 [arXiv:1001.4538 [astro-ph.CO]]; <http://lambda.gsfc.nasa.gov/product/map/current/parameters.cfm>.

- [16] G. Aad *et al.* [ATLAS Collaboration], arXiv:1109.6572 [hep-ex].
- [17] ATLAS Collaboration, <https://atlas.web.cern.ch/Atlas/GROUPS/PHYSICS/CONFNOTES/ATLAS-CONF-2011-132/ATLAS-CONF-2011-132.pdf>.
- [18] S. Chatrchyan *et al.* [CMS Collaboration], arXiv:1109.2352 [hep-ex].
- [19] CMS Collaboration, <http://cdsweb.cern.ch/record/1378096/files/HIG-11-020-pas.pdf>.
- [20] S. Chatrchyan *et al.* [CMS Collaboration], arXiv:1107.5834 [hep-ex].
- [21] R. Aaij *et al.* [LHCb Collaboration], Phys. Lett. B **699** (2011) 330 [arXiv:1103.2465 [hep-ex]]; arXiv:1112.1600 [hep-ex].
- [22] F. Gianotti for the ATLAS Collaboration, G. Tonelli for the CMS Collaboration, <http://indico.cern.ch/conferenceDisplay.py?confId=164890>.
- [23] M. Davier, A. Hoecker, B. Malaescu and Z. Zhang, Eur. Phys. J. C **71** (2011) 1515 [arXiv:1010.4180 [hep-ph]].
- [24] F. Jegerlehner and R. Szafron, Eur. Phys. J. C **71** (2011) 1632 [arXiv:1101.2872 [hep-ph]].
- [25] B. C. Allanach, Comput. Phys. Commun. **143** (2002) 305 [arXiv:hep-ph/0104145].
- [26] G. Degrossi, S. Heinemeyer, W. Hollik, P. Slavich and G. Weiglein, Eur. Phys. J. C **28** (2003) 133 [arXiv:hep-ph/0212020]; S. Heinemeyer, W. Hollik and G. Weiglein, Eur. Phys. J. C **9** (1999) 343 [arXiv:hep-ph/9812472]; S. Heinemeyer, W. Hollik and G. Weiglein, Comput. Phys. Commun. **124** (2000) 76 [arXiv:hep-ph/9812320]; M. Frank *et al.*, JHEP **0702** (2007) 047 [arXiv:hep-ph/0611326]; See <http://www.feynhiggs.de>.
- [27] T. Moroi, Phys. Rev. D **53** (1996) 6565 [Erratum-ibid. D **56** (1997) 4424] [arXiv:hep-ph/9512396].
- [28] G. Degrossi and G. F. Giudice, Phys. Rev. D **58** (1998) 053007 [arXiv:hep-ph/9803384].
- [29] S. Heinemeyer, D. Stockinger and G. Weiglein, Nucl. Phys. B **690** (2004) 62 [arXiv:hep-ph/0312264].
- [30] S. Heinemeyer, D. Stockinger and G. Weiglein, Nucl. Phys. B **699** (2004) 103 [arXiv:hep-ph/0405255].
- [31] G. Isidori and P. Paradisi, Phys. Lett. B **639** (2006) 499 [arXiv:hep-ph/0605012]; G. Isidori, F. Mescia, P. Paradisi and D. Temes, Phys. Rev. D **75** (2007) 115019 [arXiv:hep-ph/0703035], and references therein.
- [32] F. Mahmoudi, Comput. Phys. Commun. **178** (2008) 745 [arXiv:0710.2067 [hep-ph]]; Comput. Phys. Commun. **180** (2009) 1579 [arXiv:0808.3144 [hep-ph]]; D. Eriksson, F. Mahmoudi and O. Stal, JHEP **0811** (2008) 035 [arXiv:0808.3551 [hep-ph]].
- [33] S. Heinemeyer *et al.*, JHEP **0608** (2006) 052 [arXiv:hep-ph/0604147]; S. Heinemeyer, W. Hollik, A. M. Weber and G. Weiglein, JHEP **0804** (2008) 039 [arXiv:0710.2972 [hep-ph]].
- [34] G. Belanger, F. Boudjema, A. Pukhov and A. Semenov, Comput. Phys. Commun. **176** (2007) 367 [arXiv:hep-ph/0607059]; Comput. Phys. Commun. **149** (2002) 103 [arXiv:hep-ph/0112278]; Comput. Phys. Commun. **174** (2006) 577 [arXiv:hep-ph/0405253].
- [35] Information about this code is available from K. A. Olive: it contains important contributions from T. Falk, A. Ferstl, G. Ganis, A. Mustafayev, J. McDonald, K. A. Olive, P. Sandick, Y. Santoso and M. Srednicki.
- [36] P. Skands *et al.*, JHEP **0407** (2004) 036 [arXiv:hep-ph/0311123]; B. Allanach *et al.*, Comput. Phys. Commun. **180** (2009) 8 [arXiv:0801.0045 [hep-ph]].
- [37] T. Aaltonen *et al.* [CDF Collaboration], arXiv:1107.2304 [hep-ex].
- [38] J. Marrouche, private communication. For a description of DELPHES, written by S. Oryn and X. Rouby, see <http://www.fynu.ucl.ac.be/users/s.oryn/Delphes/index.html>.
- [39] E. Aprile *et al.* [XENON100 Collaboration], arXiv:1104.2549 [astro-ph.CO].